Influence of Dynamic Wireless Power Transfer on Battery Aging in Long-Haul Electric Trucks

1st Henry Winner
Technical University of Munich
Munich, Germany
henry.winner@tum.de

2nd Valentin Preis
Forschungsstelle für Energiewirtschaft
Munich, Germany
vpreis@ffe.de

3rd Felix Hell
Technical University of Munich
Munich, Germany
felix.hell@tum.de

4th Andreas Jossen
Technical University of Munich
Munich, Germany
andreas.jossen@tum.de

***Abstract*—Battery electric trucks are an opportunity to further decarbonize the road transport sector in the European Union. Due to external restrictions on driving schedules, large-capacity batteries are required in long-haul e-trucks. Dynamic wireless power transfer (DWPT) is a type of electrified road system that can charge these while driving. In this contribution, the effect of DWPT on battery aging is investigated. Synthetic driving profiles are generated from field data and then used to simulate battery aging in an e-truck. DWPT can be used to either lengthen the lifetime of the battery or to reduce battery capacity significantly without negative effects on lifetime.**

***Index Terms*—electric truck, dynamic wireless power transfer, lithium-ion, degradation, aging**

I. Introduction

Decarbonizing the road transport sector is an important goal of the European Union in its efforts to combat climate change. In [1], the CO_2 emission reduction targets for new production heavy-duty vehicles were set at $90\,\%$ for 2040 compared to the year 2019. Zero-tailpipe-emission vehicles, such as battery-electric trucks, can help in reaching that goal. Long-haul routes require drivers to spend up to $10\,\mathrm{h}$ behind the wheel, with an allowed break of $45\,\mathrm{min}$ [2]. Fulfilling this externally required schedule requires a battery capacity of $798\,\mathrm{kWh}$ as shown in [3]. Dynamic wireless power transfer (DWPT) is an electrified road system that provides power to the e-truck while it is moving. The transferred power feeds the motor and, if sufficient power is being transferred, can also charge the battery [4]. With DWPT, battery usage can be relieved, and capacity requirements can be reduced, thereby also reducing battery weight.

In this contribution, we determine the effect of DWPT on battery aging by comparing different simulation scenarios: no DWPT coverage, medium and large coverage, as well as different battery sizes and DWPT power. We focus on investigating the effects of DWPT on the following key performance indicators (KPIs): equivalent full cycles (EFCs), the average depth-of-discharge (DoD), charging and discharging C-rates, as well as lifetime to $80\,\%$ state-of-health (SoH).

This research is funded by the Federal Ministry for Economic Affairs and Energy (BMWE) via the research project EMADI (grant number 01MV23017F).

II. Methodology

A. Synthetic driving profile generation based on field data

To evaluate the impact of DWPT on battery aging in long-haul e-trucks, the recorded data from [5] is used. Over a seven-month period, 54 class N3 trucks from four German fleets were equipped with high-resolution GPS data loggers, resulting in 1.26 million km of recorded driving data. N3 trucks are heavy-duty vehicles with a gross vehicle weight of more than $12\,\mathrm{t}$, as defined by the European vehicle classification [6]. The dataset, part of the *NEFTON* research project, includes metadata of recorded trips, as well as detailed time series of vehicle speed, and was selected to represent a broad spectrum of truck operations. It contains numerous short tracks, which may correspond to vehicle repositioning or data errors. Therefore, preprocessing was performed: trips shorter than $1\,\mathrm{km}$ or lasting less than $15\,\mathrm{min}$, trips with an average speed $\leq 5\,\mathrm{km/h}$, trips exceeding $5\,\mathrm{h}$ or $500\,\mathrm{km}$, and vehicles with a daily mileage below $50\,\mathrm{km}$ were excluded. Based on this filtered dataset, generic driving profiles were generated using a Markov chain profile generator. In the model, the vehicle state at each time step is represented by a discrete-time Markov chain, with transition matrices derived from empirical logbook data specifying the probabilities of transitions between states. Fig. 1 illustrates an example of a transition matrix obtained from the applied dataset. The states considered are *rest area*, *industrial area*, and *driving*. At the end of each trip, the corresponding distance and average speed are stored according to an empirical frequency distribution. By sampling from the transition matrices, the model generates a full-year sequence of vehicle states, capturing both driving and stationary periods at specific locations. This internal model of Forschungsstelle für Energiewirtschaft will be published in the future. The Markov-based generator produced 1000 representative synthetic driving profiles for the reference year 2023, with a temporal resolution of $5\,\mathrm{min}$ intervals. According to Regulation (EG) No. 561/2006, professional drivers in the

979-8-3315-8138-1

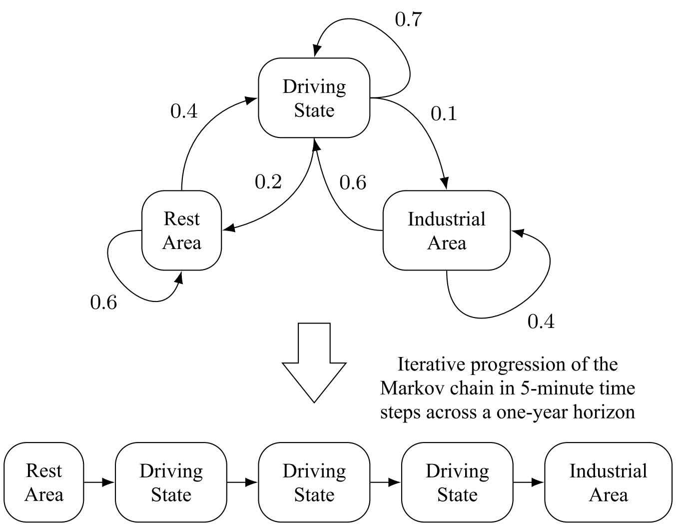

Fig. 1. **Schematic representation of the Markov process:** Example of a transition matrix that shows the transition between states, either driving or stopping at a rest stop or a depot. The goal of the Markov process was to generate synthetic driving profiles based on field data. Each state has a certain transition probability. Either it remains in the current state for the next iteration, or it moves to a different state. Each iteration represents a five-minute time step. The transition probabilities change with each iteration. The shown transition probabilities and the resulting driving profile are an example.

EU are subject to strict regulations on driving times [2]. To ensure compliance with legal driving limits, the synthetic profiles were scaled: trips exceeding the driving time before break were adjusted to $4.5\,\mathrm{h}$, and all trips were adapted to conform to the $10\,\mathrm{h}$ daily driving limit. This work focuses on long-haul e-trucks, most often driven by tractor-trailer combinations. These have an average annual kilometric performance of $110\,600\,\mathrm{km}$ while the average for all trucks stands at $23\,900\,\mathrm{km}$ [7]. Therefore, from the 1000 generated profiles, 100 with the highest annual mileage, starting at approximately $80\,000\,\mathrm{km/yr}$, were selected. The profile used for this work is a one-year profile with a total distance of $85\,580\,\mathrm{km}$. Each synthetic trip, characterized by its average speed and distance, was matched with a corresponding real trip from the dataset. The real trips include speed data sampled at $10\,\mathrm{Hz}$, which were then used in the trip energy consumption model from [8], where energy demand is calculated based on the energy required to overcome aerodynamic drag, rolling resistance, road gradient, and inertial forces. In addition, the dataset contains information on the road types for each trip segment, allowing identification of periods during which the vehicle could charge inductively on highways.

B. Simulation Environment

The open-source simulation tool SimSES [9], [10] was extended with an energy management system (EMS) for e-trucks and utilized as a simulation environment and analysis tool for battery aging KPIs. For this work, SimSES is adapted to e-trucks with DWPT technology. The driving profiles described in section II-A are processed into three profiles each. The first profile is a power profile that consists of the calculated driving power and a time stamp. The second profile, here named location profile, uses the binary profile as described by [10] and extends it to represent whether the truck is moving, at a depot, or at a rest stop. The third profile is a new binary profile that represents whether the truck is on a section of road outfitted with DWPT. The energy flows for the e-truck are shown in Fig. 2. The battery can be charged at either the depot or a rest area. Conductive charging is used for this: the AC power from the grid is converted to DC in a charging station and used to charge the battery. The energy stored in the battery is discharged through an inverter and fed into the truck's motor. The first component of the DWPT system is an AC/AC converter that converts grid power to high-frequency AC power used for the DWPT transmitter coils in the roadway. The DWPT receiver coil in the truck is connected to an AC/DC converter, which is then used to supply the inverter. Any surplus power is used to charge the battery. If the transferred power does not fulfill the drive power requirement, additional power from the battery is discharged and used.

The following parameters were defined for all simulations. The simulation duration was set to one year with a time-step resolution of $1\,\mathrm{s}$. Charging power at depots as well as at rest stops was assumed at $200\,\mathrm{kW}$. The truck battery was simulated at a system voltage of $800\,\mathrm{V}$. The AC/DC converter for conductive charging had a fixed efficiency of $85\,\%$. The DWPT path – from the electrical grid to the vehicle's motor – was defined with a total efficiency of $85\,\%$. The inverter efficiency is included in this percentage. For the inverter inside the truck, and the motor, power-dependent efficiency curves were provided. To derive these, the characteristic curves from [11] were used, where the torques were averaged for each speed and then transferred to efficiency. This was then scaled to a maximum efficiency of $95\,\%$ as shown in [12]. The battery performance and aging model by [13] was used. It is based on a Sony/Murata US266650FTC1 LFP/Graphite cell. This cell and, therefore, its aging model are not specific to e-trucks. Since the focus of this work is to compare different scenarios, and the battery remains constant, this should not affect the comparison between scenarios.

C. Scenarios

This work employs five scenarios, labeled A-E as shown in Table I. Scenario A serves as the conductive charging reference scenario; DWPT is not implemented in this scenario. A battery capacity of $800\,\mathrm{kWh}$ was chosen as a realistic battery size for long-haul e-trucks, as suggested by [3]. For scenarios B-E, a DWPT system was added. One of the main benefits of DWPT might be the possible reduction in battery capacity. In scenarios C-E, the battery capacity is therefore halved to $400\,\mathrm{kWh}$. For the considered long-haul e-trucks, this reduction in battery size corresponds to a payload increase of up to $10\,\%$. For scenarios B-D, the power of the DWPT system was chosen at $200\,\mathrm{kW}$, a realistic value for an N3 class truck as shown by Electreon's demonstrator project in France [14]. The DWPT power for scenario E was halved to investigate if the power can be reduced with full-scale deployment. Otherwise, this scenario is identical to scenario D. The DWPT-percentage

979-8-3315-8138-1

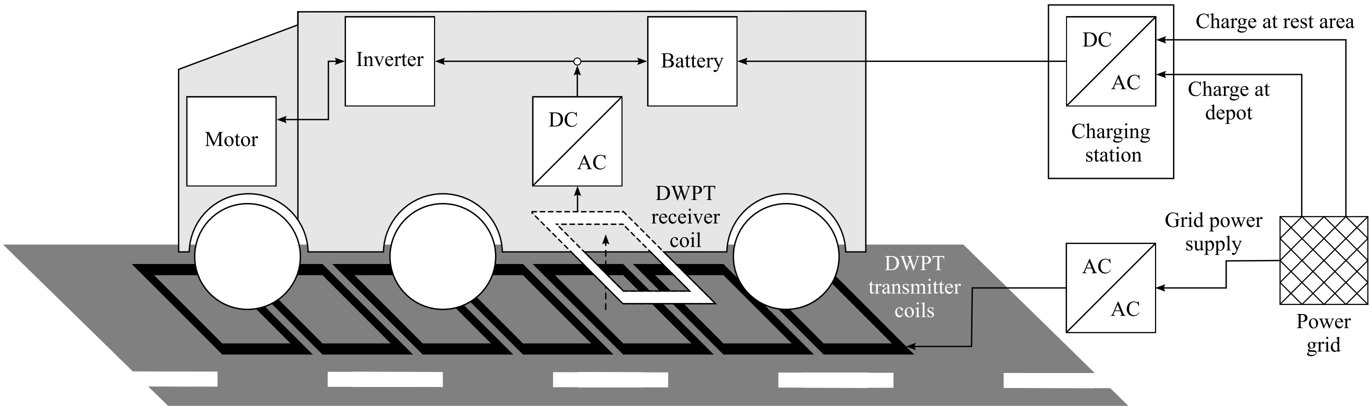

Fig. 2. **Energy flows for an e-truck equipped with DWPT:** Shown are the different possibilities to supply energy to the truck. From the power grid, the AC can either be converted to DC at a charging station and be supplied to the truck battery conductively, or it can be supplied to an AC/AC converter that feeds the DWPT transmitter coils. The transmitter coils are laid out continuously on the highway. The energy is then transferred to the DWPT receiver coil in the truck, converted to DC, and used to power the truck. This means supplying energy directly to the drive motor and also the battery if there is a surplus of energy. If there is none or not enough energy transferred via DWPT the battery is used.

is the percentage of highway kilometers driven with DWPT coverage. 40 % DWPT coverage for scenarios B and C was chosen as medium coverage. Scenarios D and E represent a full-scale deployment of DWPT at 95 % coverage.

III. Results

The full simulation results, as well as the modified version of SimSES used to obtain these, are available open-source under [15].

A. Source of energy

Fig. 3 shows the energy drawn from the power grid for the scenarios defined in Table I.

Since only one parameter is changed from scenario to scenario, a comparison between adjacent columns is justified. In the conductive reference scenario A, energy either originates from the depot (121 MWh) or a rest area (22 MWh). In scenario B, where DWPT becomes available, the share of conductive charging is reduced to 79 MWh. The DWPT share is 65 MWh and is split almost equally between going directly to the motor and charging the battery. The share of charging at rest areas is also reduced in comparison to scenario A. In scenario C, where battery capacity is halved, the total energy drawn from the grid is reduced by 8 MWh. This is due to the reduction in the truck's weight. The split between conductive charging and DWPT remains the same as in scenario B. Scenario D shows a large reduction in conductive charging.

TABLE I
Scenario Definitions

Scenario	Battery Capacity (kWh)	DWPT Power (kW)	DWPT Coverage (%)
A	800	-	-
B	800	200	40
C	400	200	40
D	400	200	95
E	400	100	95

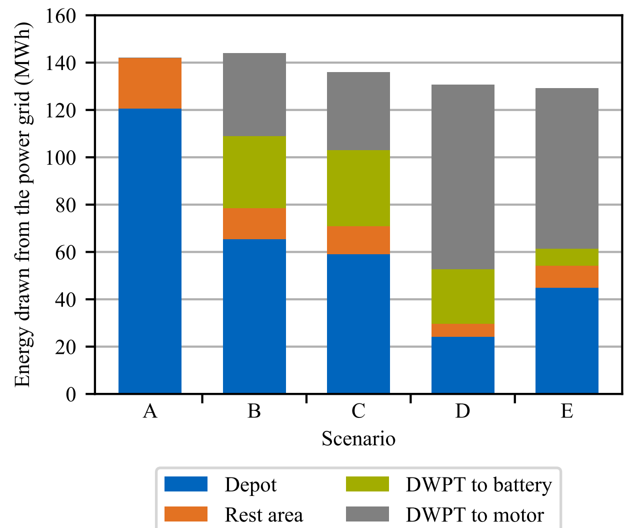

Fig. 3. **Source of the energy used by the e-truck in different scenarios:** The plot shows the energy drawn from the power grid (MWh) for the one-year, 85 580 km driving profile on the y-axis. The x-axis shows the different scenarios A-E. The colors represent the different origins of the energy used. The different scenarios A-E are defined in Table I.

It only accounts for 30 MWh, while DWPT covers the rest. The 95% DWPT coverage also means that most of the energy transferred via DWPT is directly used in the drive motor. In scenario E, where the DWPT power was halved, the energy charged conductively almost doubles to 54 MWh. Almost no energy transferred via DWPT goes to the battery; the share that goes into the motor is even larger than in scenario D.

B. Sankey diagrams

Fig. 4 depicts sankey diagrams, showing the energy flow from the power grid through all the components of the e-truck onto the road. (a) shows the conductive charging reference scenario A. Most losses occur in the AC/DC converter of the charging station. The battery incurs minimal loss, while the remaining losses originate from the inverter and motor. The

979-8-3315-8138-1

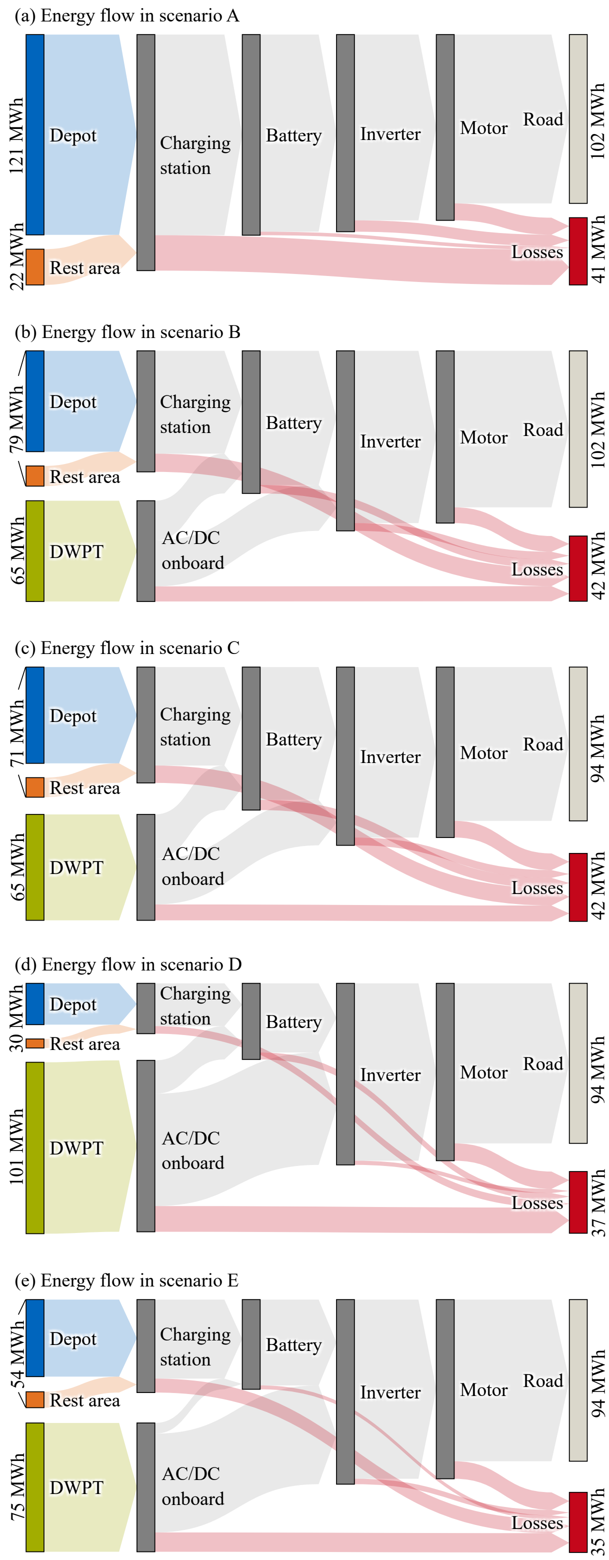

Fig. 4. **Sankey diagram of energy source, usage and loss:** Depicted are results for the one-year, 85 580 km driving profile. The energy source is depicted on the left; energy can come from a depot (blue), a rest area (orange), or via DWPT (green). The intermediate components, as introduced in Fig. 2, are depicted in dark gray. The light gray arrows represent the active energy flow through these components, while the red arrows represent losses. The subfigures (a)-(e) represent the different scenarios A-E as defined in Table I.

total losses in the entire energy storage system are 42 MWh. In comparison to that, in (b), which shows scenario B, the losses are mainly contributed by the AC/DC converter in the charging station and the losses of the energy transferred via DWPT. In the simulation, these losses are not further split into converter losses and losses that occur in the air gap. Battery, inverter, and motor losses remain largely unchanged from scenario A. Scenario C, shown in (c), has a reduced energy requirement for propulsion, as it features a lower battery capacity and therefore less e-truck weight. The losses and loss categories are also similar to scenario B. In comparison, (d) shows that scenario D has fewer overall losses at 37 MWh. The main contributors to losses are DWPT and the motor. The inverter efficiency is, as per definition in II-B, included in the DWPT efficiency. The losses from charging conductively are small, since the e-truck is powered by energy provided by DWPT. In scenario E, depicted in (e), the DWPT power is halved. This shows 2 MWh less losses than scenario D.

C. Key performance indicators for battery aging

Fig. 5 depicts KPIs for battery aging. Equivalent full cycles are shown in (a). The conductive charging reference scenario A shows that the truck's battery completes 151 EFCs in one year. Results from [10] show 37 EFCs for e-cars, 219 EFCs for e-buses, and 69 EFCs for e-boats. Long-haul trucks in Germany are typically operated by a single driver, due to the strict regulations on driving times [2]. City bus drivers are subject to the same driving time regulations, but buses can operate longer due to the ease of driver changes within urban areas. The simulation results are therefore seen as plausible. In scenario B, a significant reduction of more than 25 % in EFCs is observed. Since the energy throughput is a primary indicator of cyclic battery aging, this means that the e-truck battery in scenario B ages less than in scenario A [13]. In scenario C, where battery size is halved the EFCs almost double to 211 from 111 in scenario B . Increasing the DWPT coverage to 95 % in scenario D yields the lowest EFCs of all scenarios with 105. This is similar to scenario B, although at half the battery size. Scenario E shows a slight increase in EFCs. Because the DWPT power is halved in this scenario, more energy goes through the battery. This is also evident in Fig. 4.

The average DoD is depicted in (b). The reference scenario A shows the highest DoD of 27.7 %. This is reduced by more than 75 % when introducing DWPT in scenario B. The smaller battery in scenario C then almost doubles the DoD to 12.6 %. Increasing DWPT coverage in scenario D brings it down to a similar level as in scenario B. Scenario E has the lowest DoD at 1.3 %. This is likely due to often switching between charging and discharging the battery while driving on DWPT technology.

The average C-rate for charging is shown in (c). The trend is similar to that for DoD, although increasing DWPT coverage with a small battery does not have as large an impact. The average C-rate for discharging, as depicted in (d), is not influenced by introducing DWPT technology in scenario B. The smaller battery almost doubles this KPI, while increasing

979-8-3315-8138-1

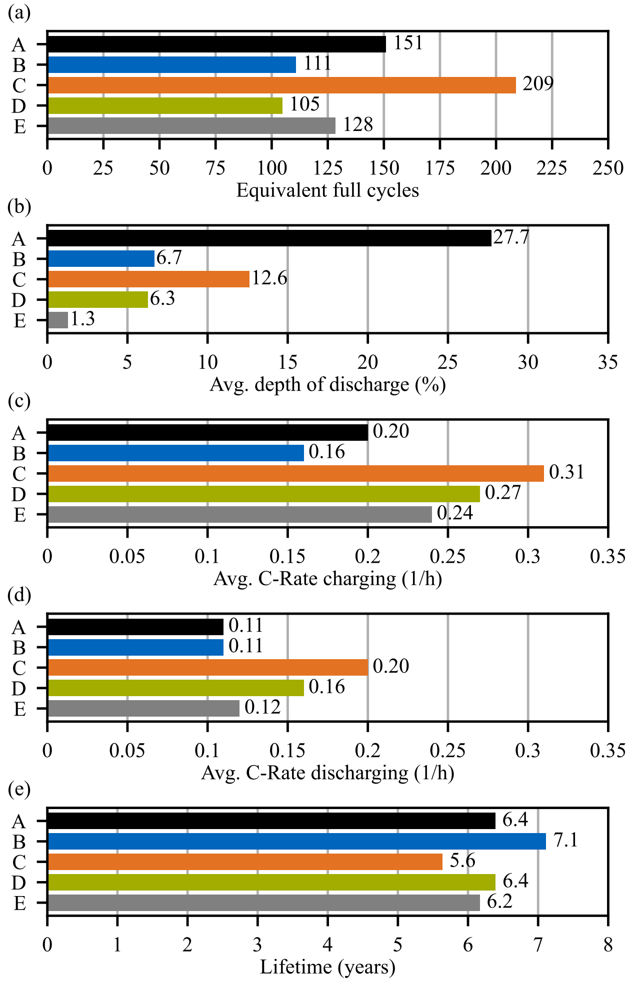

Fig. 5. **Key performance indicators for battery aging:** Depicted are results for the one-year, 85 580 km driving profile. The different scenarios A-E are defined in Table I. Subfigure (a) shows the EFCs of the e-truck battery in each scenario. The average DoD is represented in subfigure (b). Subfigures (c) and (d) depict the average charging and discharging rates, respectively. Subfigure (e) depicts the lifetime of the e-truck battery until its SoH falls below 80 %. While aging indicators in subfigures (a) - (d) were simulated in a one-year run with a high time step resolution (1 s), the lifetime was gathered from a ten-year simulation run with longer time steps (10 s).

DWPT coverage reduces it slightly. Scenario E is then almost at the same level as scenario A, likely due to the battery often needing to supply only the small surplus that the lower DWPT power is unable to deliver directly to the motor.

The lifetime of the battery is presented in (e). For the lifetime consideration, all scenarios were rerun with a 10-year time frame and a simulation timestep of 10 s. The lifetime was then extracted at 80 % SoH. The results show that introducing DWPT lengthens the lifetime of an e-truck's battery by 10 %. Reducing the battery size by half reduces the lifetime by 12.5 % compared to the reference scenario A. Scenario D shows the same lifetime as scenario A, indicating that increasing the DWPT coverage outweighs the smaller battery capacity. Scenario E has a slightly lower lifetime, indicating that the DWPT power also affects battery lifetime.

IV. Conclusion

The simulation study approach in this contribution enables the evaluation of battery aging in long-haul e-trucks through KPIs. The results show that introducing DWPT can prolong the lifetime of the e-truck battery by up to 10 %. Reducing battery capacity by 50 % with no negative effect on battery lifetime is possible with a high DWPT coverage of 95 %, which coincidentally decreases weight, allowing for either reduced energy consumption or increased transportation capacities. This decrease in weight could allow for a payload capacity up to 10 % higher.

Therefore, using DWPT technology as a means to reduce CO_2 emissions in the road transport sector seems promising.

Subjects that require further investigation include varying battery capacity, DWPT coverage, and power and conductive charging power more finely, the influence of driving profile variation on battery aging KPIs, and a close examination of CO_2 through life cycle analysis.

References

[1] "Regulation (EC) No 2019/1242 of the European Parliament and of the Council of 20 June 2019," 2019, OJ L 198 25.7.2019, p. 202. [Online]. Available: https://eur-lex.europa.eu/eli/reg/2019/1242

[2] "Regulation (EC) No 561/2006 of the European Parliament and of the Council of 15 March 2006," 2006, OJ L 102, 11.4.2006, p. 1. [Online]. Available: https://eur-lex.europa.eu/eli/reg/2006/561

[3] J. Schneider, O. Teichert, M. Zähringer, G. Balke, and M. Lienkamp, "The novel megawatt charging system standard: Impact on battery size and cell requirements for battery-electric long-haul trucks," *eTransportation*, vol. 17, p. 100253, 2023.

[4] L. Soares and H. Wang, "A study on renewed perspectives of electrified road for wireless power transfer of electric vehicles," *Renewable and Sustainable Energy Reviews*, vol. 158, p. 112110, 2022.

[5] G. Balke and L. Adenaw, "Heavy commercial vehicles' mobility: Dataset of trucks' anonymized recorded driving and operation (DT-CARGO)," *Data in Brief*, vol. 48, p. 109246, 2023.

[6] "Regulation (EU) 2018/858 of the European Parliament and of the Council of 30 May 2018," 2018, OJ L 151, 14.6.2018, pp. 1–218. [Online]. Available: https://eur-lex.europa.eu/eli/reg/2018/858

[7] M. Bäumer, H. Hautzinger, M. Pfeiffer, W. Stock, B. Lenz, T. Kuhnimhof, and K. Köhler, *Fahrleistungserhebung 2014 - Inländerfahrleistung*. Fachverlag NW in der Carl Schünemann Verlag GmbH, 2017.

[8] S. Sripad and V. Viswanathan, "Performance metrics required of next-generation batteries to make a practical electric semi truck," *ACS Energy Letters*, vol. 2, no. 7, pp. 1669–1673, 2017.

[9] M. Möller, D. Kucevic, N. Collath, A. Parlikar, P. Dotzauer, B. Tepe, S. Englberger, A. Jossen, and H. Hesse, "SimSES: A holistic simulation framework for modeling and analyzing stationary energy storage systems," *Journal of Energy Storage*, vol. 49, p. 103743, 2022.

[10] B. Tepe, S. Jablonski, H. Hesse, and A. Jossen, "Lithium-ion battery utilization in various modes of e-transportation," *eTransportation*, vol. 18, p. 100274, 2023.

[11] A. Ritari, J. Vepsäläinen, K. Kivekäs, K. Tammi, and H. Laitinen, "Energy consumption and lifecycle cost analysis of electric city buses with multispeed gearboxes," *Energies*, vol. 13, no. 8, 2020.

[12] Cascdia Motion. iM-425 integrated module. [Online]. Available: https://www.cascadiamotion.com/im-425

[13] M. Naumann, F. B. Spingler, and A. Jossen, "Analysis and modeling of cycle aging of a commercial LiFePO4/graphite cell," *Journal of Power Sources*, vol. 451, p. 227666, 2020.

[14] The EV Report. (2025) World's first wireless-charging motorway powers EVs in motion. [Online]. Available: https://theevreport.com/worlds-first-wireless-charging-motorway-powers-evs-in-motion

[15] H. Winner, V. Preis, F. Hell, and A. Jossen, "Technoeconomic analysis results of long-haul electric trucks considering dynamic wireless power transfer," 2025. [Online]. Available: https://doi.org/10.14459/2025mp1834460

979-8-3315-8138-1